Published in final edited form as:
J Mol Cell Cardiol. 2008 September ; 45(3): 420–428. doi:10.1016/j.yjmcc.2008.06.007.

Role of activated CaMKII in abnormal calcium homeostasis and I_{Na} remodeling after myocardial infarction: Insights from mathematical modeling

Thomas J. Hund[1,6], **Keith F. Decker**[2,3], **Evelyn Kanter**[4], **Peter J. Mohler**[6], **Penelope A. Boyden**[7], **Richard B. Schuessler**[1,3], **Kathryn A. Yamada**[3,4,5], and **Yoram Rudy**[2,3,4]

1*Department of Surgery Washington University in St. Louis St. Louis, MO*

2*Department of Biomedical Engineering Washington University in St. Louis St. Louis, MO*

3*Cardiac Bioelectricity and Arrhythmia Center Washington University in St. Louis St. Louis, MO*

4*Department of Medicine, Cardiovascular Division Washington University in St. Louis St. Louis, MO*

5*Center for Cardiovascular Research Washington University in St. Louis St. Louis, MO*

6*Department of Internal Medicine University of Iowa Carver College of Medicine Iowa City, IA*

7*Department of Pharmacology, Center for Molecular Therapeutics Columbia University, New York, NY 10032*

Abstract

Ca^{2+}/calmodulin-dependent protein kinase II is a multifunctional serine/threonine kinase with diverse cardiac roles including regulation of excitation contraction, transcription, and apoptosis. Dynamic regulation of CaMKII activity occurs in cardiac disease and is linked to specific disease phenotypes through its effects on ion channels, transporters, transcription and cell death pathways. Recent mathematical models of the cardiomyocyte have incorporated limited elements of CaMKII signaling to advance our understanding of how CaMKII regulates cardiac contractility and excitability. Given the importance of CaMKII in cardiac disease, it is imperative that computer models evolve to capture the dynamic range of CaMKII activity. In this study, using mathematical modeling combined with biochemical and imaging techniques, we test the hypothesis that CaMKII signaling in the canine infarct border zone (BZ) contributes to impaired calcium homeostasis and electrical remodeling. We report that the level of CaMKII autophosphorylation is significantly increased in the BZ region. Computer simulations using an updated mathematical model of CaMKII signaling reproduce abnormal Ca^{2+} transients and action potentials characteristic of the BZ. Our simulations show that CaMKII hyperactivity contributes to abnormal Ca^{2+} homeostasis and reduced action potential upstroke velocity due to effects on I_{Na} gating kinetics. In conclusion, we present a new mathematical tool for studying effects of CaMKII signaling on cardiac excitability and

Correspondence to: Thomas J. Hund; Yoram Rudy.

Address correspondence to: Thomas J. Hund Department of Internal Medicine University of Iowa Carver College of Medicine 285 Newton Road CBRB 2283 Iowa City, IA 52242 Tel:(319) 335-9679 FAX:(319) 353-5552 Email: thomas-hund@uiowa.edu Yoram Rudy Cardiac Bioelectricity and Arrhythmia Center Campus Box 1097 290 Whitaker Hall One Brookings Drive Washington University in St. Louis St. Louis, MO 63130-4899 Tel:(314) 935-8160 FAX:(314) 935-8168 Email: rudy@wustl.edu.

contractility over a dynamic range of kinase activities. Our experimental and theoretical findings establish abnormal CaMKII signaling as an important component of remodeling in the canine BZ.

Keywords

Calcium/calmodulin-dependent protein kinase II; myocardial infarction; calcium handling; mathematical modeling; arrhythmia

INTRODUCTION

Ca^{2+}/calmodulin-dependent protein kinase II (CaMKII) is a multifunctional serine/threonine kinase with diverse cardiac roles including regulation of excitation contraction, transcription, and apoptosis [1-3]. Recent findings have clearly demonstrated that dynamic regulation of CaMKII activity occurs in cardiac disease [4-12]. Aberrant CaMKII signaling has been mechanistically linked to specific disease phenotypes through its effects on a host of target proteins including ion channels and transporters, nuclear transcription factors, and cell death pathways [13-17]. For example, mice with cardiac specific CaMKII overexpression display dilated cardiomyopathy and ventricular dysfunction associated with abnormal Ca^{2+} handling [18,19] while transgenic CaMKII inhibition improves ventricular function and restores normal Ca^{2+} homeostasis after myocardial infarction [12].

Mathematical models of cardiomyocytes and cardiac tissue have been applied with great success to advance our understanding of molecular mechanisms underlying cardiac arrhythmias [20,21]. Recent models have incorporated elements of the CaMKII signaling cascade to study the role of CaMKII in regulating cardiomyocyte contractility and excitability [22-25]. Given the important role for CaMKII in cardiac disease pathogenesis, it is imperative that computer models evolve to capture the dynamic range of CaMKII activity and the functional consequences on cardiomyocyte electrical activity.

The objectives of this study are: 1) To define the activity and expression of CaMKII in the canine infarct border zone (BZ); and 2) To determine the role of CaMKII in calcium transient (CaT) and action potential (AP) remodeling in the BZ using mathematical modeling. We apply mathematical modeling combined with biochemical and imaging techniques to test the hypothesis that CaMKII signaling in the BZ contributes to impaired calcium homeostasis and electrical remodeling. We report that CaMKII activity is significantly increased in the BZ. Computer simulations show that CaMKII hyperactivity in the BZ promotes abnormal Ca^{2+} homeostasis by increasing Ca^{2+} leak from the sarcoplasmic reticulum (SR). Moreover, CaMKII hyperactivity reduces AP upstroke velocity by altering sodium current (I_{Na}) gating kinetics. In conclusion, we present a new mathematical tool for studying effects of CaMKII signaling on cardiac excitability and contractility over a dynamic activity range encompassing physiological and pathophysiological domains. Our experimental and theoretical findings establish abnormal CaMKII signaling as an important component of remodeling in the BZ.

MATERIALS AND METHODS

Mathematical model of the canine epicardial cell

The mathematical model used in this study is based on the Hund-Rudy dynamic (HRd) model of the canine epicardial cell [23]. Since first publication, new data have emerged on the function of CaMKII in heart. Here, we update our model of CaMKII signaling to account for recent findings, including CaMKII effects on I_{Na} [26] and SR Ca^{2+} leak [27]. The model uses CaMKII autophosphorylation and dephosphorylation rates slower than the original model, consistent with experimental data [28]. Revised formulation for SR calcium-induced calcium release

(CICR) that includes regulation by junctional SR Ca^{2+} and CaMKII is incorporated based on a previously published formulation [25]. Complete equations for the original HRd model and parameter values are found in a previous publication [23] and at http://rudylab.wustl.edu. Equations differing from the original may be found in the Supplement. The cell is paced from rest (initial conditions provided in Supplement) over cycle lengths from 2,000 ms to 300 ms with a conservative current stimulus [29] to steady-state (16 minutes simulated time) by applying a −80 μA/μF stimulus for a duration of 0.5 ms.

Experimental model of myocardial infarction

Myocardial infarction was produced in six healthy mongrel dogs, as described previously [30]. Infarcted hearts were isolated for subsequent analysis 4-5 days after coronary artery occlusion. BZ regions of infarcted hearts were selected from surviving epicardial tissue over the infarct. Normal regions (NZ) were selected from areas remote from the infarct. Hearts from seven non-infarcted dogs were used as controls. Experimental protocols were approved by the Animal Studies Committee at Washington University School of Medicine.

Tissue sectioning, immunoblotting and immunostaining

Serial 10 μm thick frozen sections were cut from the epicardial surface of heart samples from both BZ and remote regions. One section from each sample was prepared for immunoblotting analysis, as described previously [31]. Serial sections were placed on slides for immunohistochemistry and examined by conventional epifluorescence or laser-scanning confocal microscopy, as described previously [32]. Trichrome and hematoxylin-eosin staining was performed and analyzed to determine NZ and BZ regions of infarcted hearts (Figure 1A). Remaining slides were fixed in 4% paraformaldehyde for immunostaining.

Antibodies

Antibodies used include a rabbit polyclonal antibody (Zymed) directed against epitopes in the C-terminus of rat connexin43 (Cx43) (immunoblotting, 1:5000 dilution); a mouse monoclonal anti-Cx43 antibody (Chemicon MAB3068) (immunostaining, 1:400 dilution); rabbit polyclonal anti-phospho-CaMKII antibody directed against Thr287 (Affinity Bioreagents) (immunoblotting, 1:500; immunostaining 1:20 dilution); a custom polyclonal anti-CaMKIIδ antibody directed against the C-terminal sequence (generous gift of Dr. DM Bers) [33] (immunoblotting, 1:6000); and a polyclonal anti-actin antibody (Santa Cruz) (immunoblotting, 1:1000 dilution). Densitometric measurements for immunoblots were normalized to actin.

Statistics

When appropriate, differences between groups were analyzed with ANOVA and Tukey test. A value of $p<0.05$ was considered statistically significant. Values are expressed as mean ± SD.

RESULTS

Levels of CaMKII PThr287 are increased in the BZ

Experiments were first conducted to define CaMKII levels and activity in the BZ. Trichrome-stained sections (Figure 1A) reveal gross tissue structure of a control sample from a non-infarcted heart and NZ and BZ epicardial samples from an infarcted heart. In BZ, viable myocytes are arranged in a disorganized fashion due to presence of underlying infarct and increased collagen deposition (*blue* staining Figure 1A, *right panel*). Immunoblots from control, NZ, and BZ heart samples are shown in Figure 1B (*left*). Densitometric measurements (normalized to actin, Figure 1B, *right*) reveal a greater than 2-fold increase in levels of CaMKII phosphorylated at Thr287 (autophosphorylation site; CaMKII PThr287) in BZ compared to NZ or control, without any significant change in total CaMKII expression.

Updated mathematical model of CaMKII regulation

To determine the role of CaMKII hyperactivity in BZ, we applied our updated mathematical model of the normal epicardial canine myocyte. Steady-state APs and CaTs generated by the control (NZ) model are shown in Figure 2A. CaMKII hyperactivity (100% active subunits) shifts I_{Na} availability in the hyperpolarizing direction (Figure 2B), delays recovery from I_{Na} inactivation (Figure 2C), and increases the magnitude of the late Na^+ current (Figure 2D) [26]. Consistent with experimental measurements [26], CaMKII hyperactivity does not affect activation in the model (not shown). CaMKII-dependence of SR Ca^{2+} leak was formulated so that maximal activation produces a similar decrease in SR Ca^{2+} content as measured in myocytes overexpressing CaMKIIδ (Figure 2E) [27]. CaMKII-dependence of $I_{Ca(L)}$ was updated so that maximal CaMKII activity produces a similar slowing of inactivation and increase in peak current (Supplement Fig. S1) as measured in myocytes overexpressing CaMKIIδ [27]. The model also includes CaMKII effects on I_{rel} and SR Ca^{2+} uptake via phospholamban as previously published [23, 25].

Mathematical model of BZ myocyte simulates remodeled Ca^{2+} transients and I_{Na}

To create a mathematical model of the BZ, several major ion channel remodeling changes were incorporated into our model (summarized in Figure 3A), including a 36% reduction in $I_{Ca(L)}$ permeability [34], 60% reduction in the conductance of I_{Na} [35], elimination of I_{to} [36] and reduction of I_{K1} [36]. To simulate CaMKII hyperactivity in BZ, the CaMKII autophosphorylation rate was increased to activate CaMKII more than twofold over normal levels at baseline, consistent with our measurements (Figure 3B). The BZ model with CaMKII hyperactivity displays a hyperpolarizing shift in I_{Na} availability (−4.3 mV compared to −3.7 mV measured experimentally [35]) and slowing of recovery from inactivation (by 45% compared to 32.6% measured experimentally [35]). Note that changes to I_{Na} kinetics in the BZ model are downstream of CaMKII hyperactivity. Simulated steady-state APs and CaTs in NZ and BZ myocytes are shown in Figure 3C. Compared to NZ, the BZ AP displays diminished amplitude, lacks a phase-1 repolarization notch, and is more triangular in shape, while the CaT has diminished amplitude (CaT_{amp}), consistent with experimental measurements [36-38]. Parameters for the BZ model that differ from the updated HRd model of the NZ myocyte (Figure 2) are provided in the Supplement.

Previously, it has been reported that CaT_{amp} rate dependence is abnormal in BZ [38]. Therefore, we paced the NZ and BZ models over a range of pacing frequencies and analyzed changes in CaT and AP. Simulated (*right*) and experimentally measured [38] (*left*) CaTs are shown at slow and rapid pacing in Figure 4A. As pacing frequency increases (up until ˜2.0 Hz), NZ CaT_{amp} increases (Figure 4B, *black line*). In contrast, BZ CaT_{amp} shows a negative dependence on pacing frequency (Figure 4B, *gray line*), consistent with experiments [38]. AP duration (APD) also shows abnormal response to pacing frequency in the BZ model. As pacing rate increases, the BZ AP transitions from being slightly shorter to slightly longer than NZ, revealing a decreased capacity for APD adaptation (Figure 4C). Finally, maximal action potential upstroke velocity (dV/dt_{max}) is much slower in BZ than NZ at all frequencies (Figure 4D).

Role of CaMKII in BZ calcium transient and action potential remodeling

To examine the role of CaMKII in BZ remodeling, we analyzed the dependence of steady-state CaT_{amp} (Figure 5A), dV/dt_{max} (Figure 5B), and APD (not shown) on basal CaMKII activity (pacing frequency = 1 Hz). Basal CaMKII activity was altered by changing CaMKII autophosphorylation rate. Interestingly, CaT_{amp} shows a biphasic dependence on CaMKII activity in NZ and BZ models (Figure 5A). For moderate activity levels, CaMKII positively regulates CaT_{amp}. However, more severe CaMKII hyperactivity impairs intracellular Ca^{2+} cycling reflected as decreased CaT_{amp}. Default CaMKII activity levels for NZ and BZ models

are shown on the curves as reference points (Figure 5, *open circles*). Notice that the BZ model operates in the domain where CaMKII is detrimental to Ca^{2+} cycling. Effects of CaMKII activity on the AP were also analyzed. CaMKII activation slows the action potential upstroke in both NZ and BZ models (Figure 5B) but has little effect on APD (< 3% change from default values, data not shown).

To elucidate the mechanism by which CaMKII hyperactivity impairs intracellular Ca^{2+} cycling in BZ, cytosolic (Figure 6A) and SR (Figure 6B) Ca^{2+} concentrations, and Ca^{2+} currents and fluxes targeted by CaMKII (Figure 6B-F) during steady state pacing (frequency = 1 Hz) are compared in the BZ model (Figure 6, *gray line*) and the BZ model with CaMKII activity restored to normal levels (Figure 6, *black line*). CaMKII hyperactivity increases diastolic SR Ca^{2+} leak (Figure 6C), which decreases junctional SR Ca^{2+} (Figure 6B) leading to reduced calcium-induced calcium release (CICR) from the SR (Figure 6F). Decreased junctional SR Ca^{2+} and CICR occur despite the fact that CaMKII hyperactivity increases peak L-type Ca^{2+} current (Figure 6D) and SR Ca^{2+} uptake (Figure 6E).

The mechanism by which CaMKII hyperactivity reduces maximal upstroke velocity in BZ was also examined by comparing I_{Na} properties in the BZ model (Figure 7, *gray*) and the BZ model with CaMKII restored to normal levels (Figure 7, *black*). CaMKII hyperactivity decreases peak I_{Na} during pacing (increased use dependence, Figure 7B) due to a depolarizing shift in channel availability (Figure 7C) and a slowing of recovery from inactivation (Figure 7D).

While our model predicts that CaMKII hyperactivity contributes to remodeling of the CaT and AP upstroke, it does not support a role for CaMKII in abnormal APD adaptation. Instead, our model predicts that downregulation of I_{to} and to a lesser extent $I_{Ca(L)}$ reduces the capacity for APD adaptation in BZ (Supplement Figure S3). This is illustrated in simulations where adaptation (change in APD as pacing frequency decreases from 2.0 Hz to 0.5 Hz) was compared in the following models: NZ, BZ, BZ with normal I_{to} density, and BZ with normal $I_{Ca(L)}$ density (Supplement Figure S3A). Restoring normal I_{to} density almost completely recovered normal APD adaptation. It is also important to note that while CaMKII hyperactivity contributes to reduced AP upstroke velocity by altering I_{Na} gating kinetics, our model predicts that downregulation of peak current density (reflecting channel expression) accounts for a large portion of the reduction in upstroke velocity observed in BZ (Supplement Figure S3B).

DISCUSSION

In this study, we use mathematical modeling to link CaMKII hyperactivity measured in the BZ to abnormal calcium homeostasis and I_{Na} remodeling. While previous modeling studies have examined electrophysiological consequences of ion channel remodeling in the BZ [39,40], our effort represents a novel approach where acute effects downstream of aberrant cell signaling are studied over a dynamic activity range encompassing normal and pathological domains. Our new data point to a critical role for CaMKII in adverse remodeling after myocardial infarction.

Coronary heart disease is the number one killer in the United States with ventricular fibrillation thought to be responsible for the majority of sudden deaths [41]. The need is great, therefore, to develop new and more effective therapies for treating patients with coronary heart disease. While molecular mechanisms responsible for remodeling and increased arrhythmia susceptibility after myocardial infarction are not fully understood, it is clear that dramatic remodeling of ion channels occurs in the BZ [34-36,42,43] creating a substrate favorable to initiation and maintenance of reentrant arrhythmias. Upstream cell signaling pathways responsible for triggering remodeling post-MI represent a new class of potential therapeutic targets for preventing arrhythmias [44,45]. The importance of CaMKII signaling in heart disease has been established by important studies from several independent groups (reviewed

in detail [2,44]). CaMKII upregulation has been documented in hypertrophy and heart failure [4-8,18], including human dilated cardiomyopathy [9]. Furthermore, transgenic overexpression of CaMKIIδ promotes hypertrophy and heart failure in mice [19,46], while CaMKII inhibition prevents left ventricular remodeling and restores normal Ca^{2+} homeostasis in the infarcted mouse heart [12]. Finally, CaMKII inhibition in a transgenic mouse model of cardiac hypertrophy prevents cardiac arrhythmias [47]. Results of our computer simulations reveal that SR calcium leak due to CaMKII hyperphosphorylation depletes SR Ca^{2+} content and contributes to depressed calcium transients. The role of SR Ca^{2+} leak in cardiac disease and arrhythmia is unclear, although enhanced SR Ca^{2+} leak has been proposed as an important arrhythmogenic factor in the setting of either acquired or congenital ryanodine receptor dysfunction (see review [48]).

Our simulations also reveal that CaMKII hyperactivity in the BZ alters I_{Na} gating, contributing to reduced maximum upstroke velocity observed in the model as well as in cells isolated from the BZ [36]. Increased post-repolarization refractoriness in the BZ, attributed to I_{Na} remodeling, has been proposed as a mechanism for slow conduction and arrhythmogenesis [39]. Therefore, our data suggest that CaMKII hyperactivity may not only impair Ca^{2+} homeostasis but also conduction, thereby promoting formation of the substrate required for initiation and maintenance of lethal cardiac arrhythmias.

It is important to consider the possibility that cardiac disease may regulate the subcellular distribution of CaMKII. To address the possibility of CaMKII subcellular localization changes in BZ, tissue sections were immunostained and analyzed by confocal microscopy. Figure 8 shows CaMKII PThr287 (red, *far left*), connexin43 (green, *left of center*), and merged images (*right of center*) from control (*top*) and BZ (*bottom*) sections. Increased CaMKII PThr287 immunoreactive signal is evident in BZ compared to control, consistent with immunoblotting data in Figure 1. Interestingly, increased CaMKII PThr287 is most apparent at cell ends in the area of the intercalated disc marked by prominent Cx43 staining (Figure 8, *arrow*). It is intriguing to consider the possibility that Na^+ channels may be targets for CaMKII at the intercalated disc [49]. In the cardiomyocyte, Na^+ channels are found at the sarcolemma and t-tubules but are concentrated at the intercalated disc where neighboring cells are in close apposition [50-54]. Importantly, it has been shown that BZ cells retain Na^+ channel localization at the intercalated disc [49]. Recent studies report that direct phosphorylation of Na^+ channels by CaMKII dramatically alters channel gating [26], while previous modeling studies have shown that clustering of Na^+ channels at the intercalated disc has important consequences for cell excitability and conduction [51]. It will be interesting for future modeling studies to address the electrophysiological consequences of preferential phosphorylation of Na^+ channels at the intercalated disc region. It is also important to consider that CaMKII is likely compartmentalized into functional subcellular domains (Figure 8). Additional quantitative experimental data are needed on the subcellular distribution of CaMKII and how this changes with disease. With these additional data, more advanced mathematical models of CaMKII activity may be integrated into detailed models of SR CICR [55-58] to generate new insight into the regulation of cell contractility and excitability.

Limitations of the model

Remodeling in the BZ is a complex process characterized by both mechanical and electrical remodeling. While our study focuses on the role of CaMKII, there are likely many factors responsible for triggering remodeling in the BZ. More detailed models of the BZ reflecting changes in the three-dimensional structure of the tissue will yield important new insights. It is also important to note that while our mathematical model of CaMKII regulation accounts for many known CaMKII targets, there remain others to be included in the future (K^+ channels

[22,59,60], for example). Our model provides a dynamic framework into which these targets may be integrated.

Supplementary Material

Refer to Web version on PubMed Central for supplementary material.

ACKNOWLEDGMENTS

This study was supported by NIH Grant R01-HL49054 and NIH MERIT Award R37-HL33343 (to YR), HL66350 (to KY), HL083422 (PJM), HL084979 (TJH), HL66140 (PAB) and by a University of Iowa Cardiovascular Interdisciplinary Research Fellowship NIH T32 HL00731 (TJH). Y. Rudy is the Fred Saigh Distinguished Professor at Washington University.

REFERENCES

[1]. Braun AP, Schulman H. The multifunctional calcium/calmodulin-dependent protein kinase: from form to function. Annu Rev Physiol 1995;57:417–45. [PubMed: 7778873]

[2]. Hund TJ, Rudy Y. A role for calcium/calmodulin-dependent protein kinase II in cardiac disease and arrhythmia. Handb Exp Pharmacol 2006;171:201–20. [PubMed: 16610345]

[3]. Maier LS, Bers DM. Calcium, calmodulin, and calcium-calmodulin kinase II: heartbeat to heartbeat and beyond. J Mol Cell Cardiol 2002;34(8):919–39. [PubMed: 12234763]

[4]. Boknik P, Heinroth-Hoffmann I, Kirchhefer U, Knapp J, Linck B, Luss H, et al. Enhanced protein phosphorylation in hypertensive hypertrophy. Cardiovasc Res Sep;2001 51(4):717–28. [PubMed: 11530105]

[5]. Colomer JM, Mao L, Rockman HA, Means AR. Pressure overload selectively up-regulates Ca^{2+}/calmodulin-dependent protein kinase II *in vivo*. Mol Endocrinol Feb;2003 17(2):183–92. [PubMed: 12554746]

[6]. Currie S, Smith GL. Calcium/calmodulin-dependent protein kinase II activity is increased in sarcoplasmic reticulum from coronary artery ligated rabbit hearts. FEBS Lett Oct 8;1999 459(2): 244–8. [PubMed: 10518028]

[7]. Hagemann D, Bohlender J, Hoch B, Krause EG, Karczewski P. Expression of Ca^{2+}/calmodulin-dependent protein kinase II δ-subunit isoforms in rats with hypertensive cardiac hypertrophy. Mol Cell Biochem Apr;2001 220(12):69–76. [PubMed: 11451385]

[8]. Hempel P, Hoch B, Bartel S, Karczewski P. Hypertrophic phenotype of cardiac calcium/calmodulin-dependent protein kinase II is reversed by angiotensin converting enzyme inhibition. Basic Res Cardiol 2002;97(Supp 1):I96–101. [PubMed: 12479242]

[9]. Hoch B, Meyer R, Hetzer R, Krause EG, Karczewski P. Identification and expression of δ-isoforms of the multifunctional Ca^{2+}/calmodulin-dependent protein kinase in failing and nonfailing human myocardium. Circ Res 1999;84(6):713–21. [PubMed: 10189359]

[10]. Mishra S, Sabbah HN, Jain JC, Gupta RC. Reduced Ca^{2+}-calmodulin-dependent protein kinase activity and expression in LV myocardium of dogs with heart failure. Am J Physiol Heart Circ Physiol 2003;284(3):H876–83. [PubMed: 12424092]

[11]. Netticadan T, Temsah RM, Kawabata K, Dhalla NS. Sarcoplasmic reticulum Ca^{2+}/Calmodulin-dependent protein kinase is altered in heart failure. Circ Res 2000;86(5):596–605. [PubMed: 10720422]

[12]. Zhang R, Khoo MS, Wu Y, Yang Y, Grueter CE, Ni G, et al. Calmodulin kinase II inhibition protects against structural heart disease. Nat Med Mar 27;2005 11:409–17. [PubMed: 15793582]

[13]. Bossuyt J, Helmstadter K, Wu X, Clements-Jewery H, Haworth RS, Avkiran M, et al. Ca^{2+}/Calmodulin-Dependent Protein Kinase IIδ and Protein Kinase D Overexpression Reinforce the Histone Deacetylase 5 Redistribution in Heart Failure. Circ Res. Jan 24;2008

[14]. Passier R, Zeng H, Frey N, Naya FJ, Nicol RL, McKinsey TA, et al. CaM kinase signaling induces cardiac hypertrophy and activates the MEF2 transcription factor in vivo. J Clin Invest May;2000 105(10):1395–406. [PubMed: 10811847]

[15]. Zhu W, Woo AY, Yang D, Cheng H, Crow MT, Xiao RP. Activation of CaMKII-delta C is a common intermediate of diverse death stimuli-induced heart muscle cell apoptosis. J Biol Chem. Feb 12;2007

[16]. Zhu WZ, Wang SQ, Chakir K, Yang D, Zhang T, Brown JH, et al. Linkage of β1-adrenergic stimulation to apoptotic heart cell death through protein kinase A-independent activation of Ca^{2+}/calmodulin kinase II. J Clin Invest Mar;2003 111(5):617–25. [PubMed: 12618516]

[17]. Ramirez MT, Zhao XL, Schulman H, Brown JH. The nuclear δ_B isoform of Ca^{2+}/calmodulin-dependent protein kinase II regulates atrial natriuretic factor gene expression in ventricular myocytes. J Biol Chem Dec 5;1997 272(49):31203–8. [PubMed: 9388275]

[18]. Zhang T, Maier LS, Dalton ND, Miyamoto S, Ross J Jr. Bers DM, et al. The δ_C isoform of CaMKII is activated in cardiac hypertrophy and induces dilated cardiomyopathy and heart failure. Circ Res 2003;92:912–9. [PubMed: 12676814]

[19]. Maier LS, Zhang T, Chen L, DeSantiago J, Brown JH, Bers DM. Transgenic CaMKIIδ_C overexpression uniquely alters cardiac myocyte Ca^{2+} handling: reduced SR Ca^{2+} load and activated SR Ca^{2+} release. Circ Res May 2;2003 92(8):904–11. [PubMed: 12676813]

[20]. Noble D, Rudy Y. Models of cardiac ventricular action potentials: iterative interaction between experiment and simulation. Philos Trans R Soc Lond A 2001;359:1127–42.

[21]. Rudy Y, Silva JR. Computational biology in the study of cardiac ion channels and cell electrophysiology. Q Rev Biophys Feb;2006 39(1):57–116. [PubMed: 16848931]

[22]. Grandi E, Puglisi JL, Wagner S, Maier LS, Severi S, Bers DM. Simulation of Ca-Calmodulin-Dependent Protein Kinase II on Rabbit Ventricular Myocyte Ion Currents and Action Potentials. Biophys J Dec 1;2007 93(11):3835–47. [PubMed: 17704163]

[23]. Hund TJ, Rudy Y. Rate dependence and regulation of action potential and calcium transient in a canine cardiac ventricular cell model. Circulation 2004;110:3168–74. [PubMed: 15505083]

[24]. Iribe G, Kohl P, Noble D. Modulatory effect of calmodulin-dependent kinase II (CaMKII) on sarcoplasmic reticulum Ca^{2+} handling and interval-force relations: a modelling study. Philos Transact A Math Phys Eng Sci May 15;2006 364(1842):1107–33. [PubMed: 16608699]

[25]. Livshitz LM, Rudy Y. Regulation of Ca^{2+} and electrical alternans in cardiac myocytes: Role of CaMKII and repolarizing currents. Am J Physiol Heart Circ Physiol Feb 2;2007 292:H2854–H66. [PubMed: 17277017]

[26]. Wagner S, Dybkova N, Rasenack EC, Jacobshagen C, Fabritz L, Kirchhof P, et al. Ca/calmodulin-dependent protein kinase II regulates cardiac Na channels. J Clin Invest Dec 1;2006 116(12):3127–38. [PubMed: 17124532]

[27]. Kohlhaas M, Zhang T, Seidler T, Zibrova D, Dybkova N, Steen A, et al. Increased sarcoplasmic reticulum calcium leak but unaltered contractility by acute CaMKII overexpression in isolated rabbit cardiac myocytes. Circ Res Feb 3;2006 98(2):235–44. [PubMed: 16373600]

[28]. Gaertner TR, Kolodziej SJ, Wang D, Kobayashi R, Koomen JM, Stoops JK, et al. Comparative analyses of the three-dimensional structures and enzymatic properties of α, β, γ and δ isoforms of Ca^{2+}-calmodulin-dependent protein kinase II. J Biol Chem Mar 26;2004 279(13):12484–94. [PubMed: 14722083]

[29]. Hund TJ, Kucera JP, Otani NF, Rudy Y. Ionic charge conservation and long-term steady state in the Luo-Rudy dynamic model of the cardiac cell. Biophys J 2001;81(6):3324–31. [PubMed: 11720995]

[30]. Nitta T, Schuessler RB, Mitsuno M, Rokkas CK, Isobe F, Cronin CS, et al. Return cycle mapping after entrainment of ventricular tachycardia. Circulation Mar 31;1998 97(12):1164–75. [PubMed: 9537343]

[31]. Johnson CM, Kanter EM, Green KG, Laing JG, Betsuyaku T, Beyer EC, et al. Redistribution of connexin45 in gap junctions of connexin43-deficient hearts. Cardiovasc Res Mar;2002 53(4):921–35. [PubMed: 11922902]

[32]. Kwong KF, Schuessler RB, Green KG, Laing JG, Beyer EC, Boineau JP, et al. Differential expression of gap junction proteins in the canine sinus node. Circ Res Mar 23;1998 82(5):604–12. [PubMed: 9529165]

[33]. Huke S, Bers DM. Temporal dissociation of frequency-dependent acceleration of relaxation and protein phosphorylation by CaMKII. J Mol Cell Cardiol. Dec 21;2006

[34]. Aggarwal R, Boyden PA. Diminished Ca^{2+} and Ba^{2+} currents in myocytes surviving in the epicardial border zone of the 5-day infarcted canine heart. Circ Res 1995;77(6):1180–91. [PubMed: 7586231]

[35]. Pu J, Boyden PA. Alterations of Na^{+} currents in myocytes from epicardial border zone of the infarcted heart. A possible ionic mechanism for reduced excitability and postrepolarization refractoriness. Circ Res 1997;81(1):110–9. [PubMed: 9201034]

[36]. Lue WM, Boyden PA. Abnormal electrical properties of myocytes from chronically infarcted canine heart. Alterations in V_{max} and the transient outward current. Circulation 1992;85(3):1175–88. [PubMed: 1371431]

[37]. Ursell PC, Gardner PI, Albala A, Fenoglio JJ Jr. Wit AL. Structural and electrophysiological changes in the epicardial border zone of canine myocardial infarcts during infarct healing. Circ Res 1985;56 (3):436–51. [PubMed: 3971515]

[38]. Licata A, Aggarwal R, Robinson RB, Boyden P. Frequency dependent effects on Ca_i transients and cell shortening in myocytes that survive in the infarcted heart. Cardiovasc Res 1997;33(2):341–50. [PubMed: 9074698]

[39]. Cabo C, Boyden P. Electrical remodeling of the epicardial border zone in the canine infarcted heart: a computational analysis. Am J Physiol Heart Circ Physiol 2003;284:H372–H84. [PubMed: 12388240]

[40]. Cabo C, Yao J, Boyden PA, Chen S, Hussain W, Duffy HS, et al. Heterogeneous gap junction remodeling in reentrant circuits in the epicardial border zone of the healing canine infarct. Cardiovasc Res Nov 1;2006 72(2):241–9. [PubMed: 16914125]

[41]. Heart Disease and Stroke Statistics - 2007 Update: American Heart Association. 2007.

[42]. Jiang M, Cabo C, Yao JA, Boyden PA, Tseng GN. Delayed rectifier K currents have reduced amplitudes and altered kinetics in myocytes from infarcted canine ventricle. Cardiovasc Res 2000;48(1):34–43. [PubMed: 11033106]

[43]. Peters NS, Coromilas J, Severs NJ, Wit AL. Disturbed connexin43 gap junction distribution correlates with the location of reentrant circuits in the epicardial border zone of healing canine infarcts that cause ventricular tachycardia. Circulation 1997;95(4):988–96. [PubMed: 9054762]

[44]. Anderson ME. Multiple downstream proarrhythmic targets for calmodulin kinase II: moving beyond an ion channel-centric focus. Cardiovasc Res Mar 1;2007 73(4):657–66. [PubMed: 17254559]

[45]. Hund TJ, Saffitz JE. Is CaMKII a therapeutic target for ventricular rate control? Heart Rhythm Jun; 2005 2(6):641–2. [PubMed: 15922274]

[46]. Zhang T, Johnson EN, Gu Y, Morissette MR, Sah VP, Gigena MS, et al. The cardiac-specific nuclear δ_B isoform of Ca^{2+}/calmodulin-dependent protein kinase II induces hypertrophy and dilated cardiomyopathy associated with increased protein phosphatase 2A activity. J Biol Chem Jan 11;2002 277(2):1261–7. [PubMed: 11694533]

[47]. Wu Y, Temple J, Zhang R, Dzhura I, Zhang W, Trimble R, et al. Calmodulin kinase II and arrhythmias in a mouse model of cardiac hypertrophy. Circulation Sep 3;2002 106(10):1288–93. [PubMed: 12208807]

[48]. Sobie EA, Guatimosim S, Gomez-Viquez L, Song LS, Hartmann H, Saleet Jafri M, et al. The Ca^{2+} leak paradox and rogue ryanodine receptors: SR Ca^{2+} efflux theory and practice. Prog Biophys Mol Biol Jan-Apr;2006 90(13):172–85. [PubMed: 16326215]

[49]. Baba S, Dun W, Cabo C, Boyden PA. Remodeling in cells from different regions of the reentrant circuit during ventricular tachycardia. Circulation Oct 18;2005 112(16):2386–96. [PubMed: 16203911]

[50]. Cohen SA. Immunocytochemical localization of rH1 sodium channel in adult rat heart atria and ventricle. Presence in terminal intercalated disks. Circulation Dec 15;1996 94(12):3083–6. [PubMed: 8989112]

[51]. Kucera JP, Rohr S, Rudy Y. Localization of sodium channels in intercalated disks modulates cardiac conduction. Circ Res Dec 13;2002 91(12):1176–82. [PubMed: 12480819]

[52]. Maier SK, Westenbroek RE, Schenkman KA, Feigl EO, Scheuer T, Catterall WA. An unexpected role for brain-type sodium channels in coupling of cell surface depolarization to contraction in the heart. Proc Natl Acad Sci U S A Mar 19;2002 99(6):4073–8. [PubMed: 11891345]

[53]. Mohler PJ, Rivolta I, Napolitano C, LeMaillet G, Lambert S, Priori SG, et al. Nav1.5 E1053K mutation causing Brugada syndrome blocks binding to ankyrin-G and expression of Nav1.5 on the surface of cardiomyocytes. Proc Natl Acad Sci U S A Dec 14;2004 101(50):17533–8. [PubMed: 15579534]

[54]. Scriven DR, Dan P, Moore ED. Distribution of proteins implicated in excitation-contraction coupling in rat ventricular myocytes. Biophys J 2000;79(5):2682–91. [PubMed: 11053140]

[55]. Greenstein JL, Winslow RL. An integrative model of the cardiac ventricular myocyte incorporating local control of Ca^{2+} release. Biophys J 2002;83(6):2918–45. [PubMed: 12496068]

[56]. Shannon TR, Wang F, Puglisi J, Weber C, Bers DM. A mathematical treatment of integrated Ca dynamics within the ventricular myocyte. Biophys J Nov;2004 87(5):3351–71. [PubMed: 15347581]

[57]. Sobie EA, Dilly KW, dos Santos Cruz J, Lederer WJ, Jafri MS. Termination of cardiac Ca^{2+} sparks: an investigative mathematical model of calcium-induced calcium release. Biophys J 2002;83(1): 59–78. [PubMed: 12080100]

[58]. Faber GM, Silva J, Livshitz L, Rudy Y. Kinetic properties of the cardiac L-type Ca^{2+} channel and its role in myocyte electrophysiology: a theoretical investigation. Biophys J Mar 1;2007 92(5): 1522–43. [PubMed: 17158566]

[59]. Li J, Marionneau C, Zhang R, Shah V, Hell JW, Nerbonne JM, et al. Calmodulin kinase II inhibition shortens action potential duration by upregulation of K^+ currents. Circ Res Nov 10;2006 99(10): 1092–9. [PubMed: 17038644]

[60]. Tessier S, Karczewski P, Krause EG, Pansard Y, Acar C, Lang-Lazdunski M, et al. Regulation of the transient outward K^+ current by Ca^{2+}/calmodulin-dependent protein kinases II in human atrial myocytes. Circ Res 1999;85(9):810–9. [PubMed: 10532949]

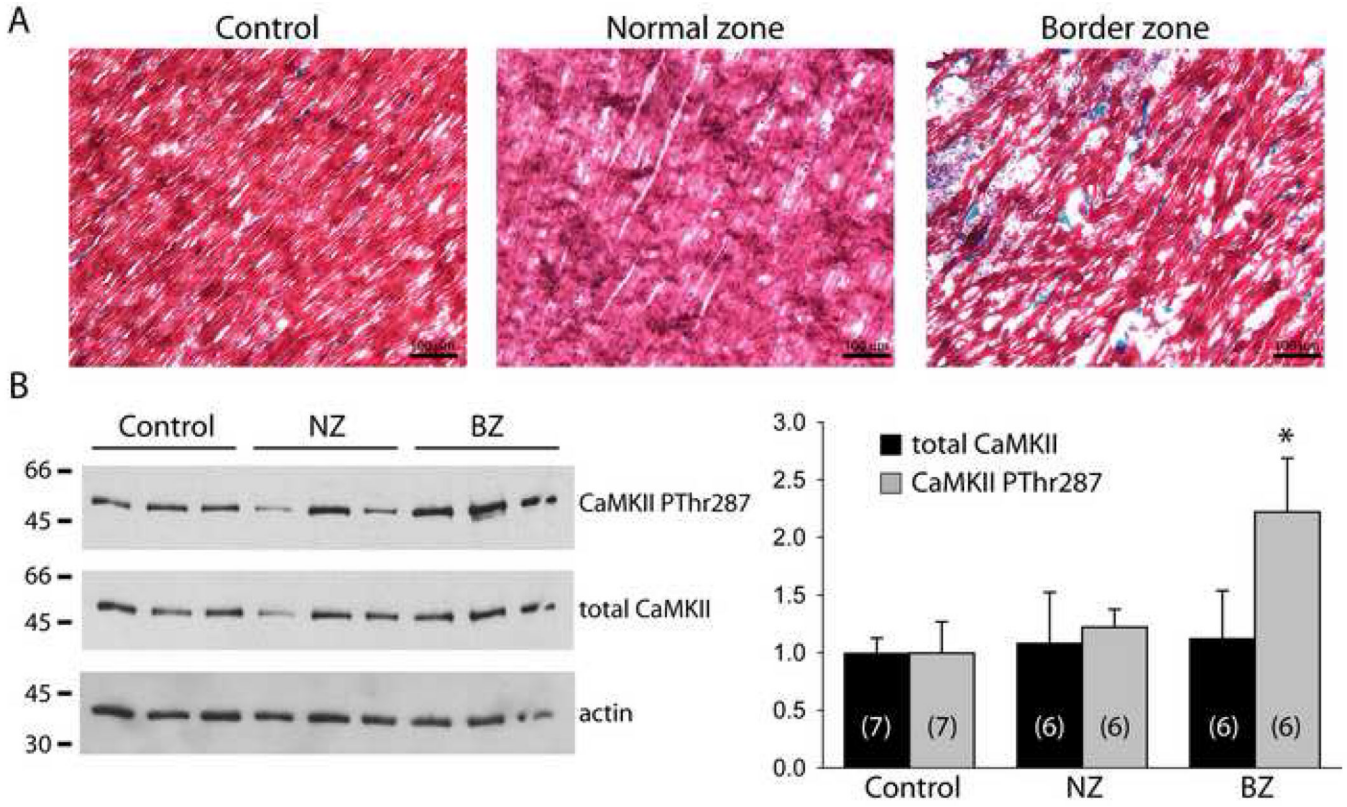

FIGURE 1. Experimental measurement of autophosphorylated and total CaMKII in the infarct border zone

(**A**) Representative epicardial trichrome-stained sections from control, normal zone, and infarct border zone (BZ) samples. Blue staining indicates presence of collagen deposition. (**B**) Immunoblots (*left*) and densitometric measurements (*right*) of CaMKII phosphorylated at the autophosphorylation site Thr287 (CaMKII PThr287), total CaMKII and actin protein levels in control, normal zone (NZ), and infarct border zone (BZ) samples. Error bars designate standard deviation. (*$p<0.01$ vs. NZ or control, sample size for each group indicated in respective bars: n = 7 for control, n = 6 for NZ and BZ).

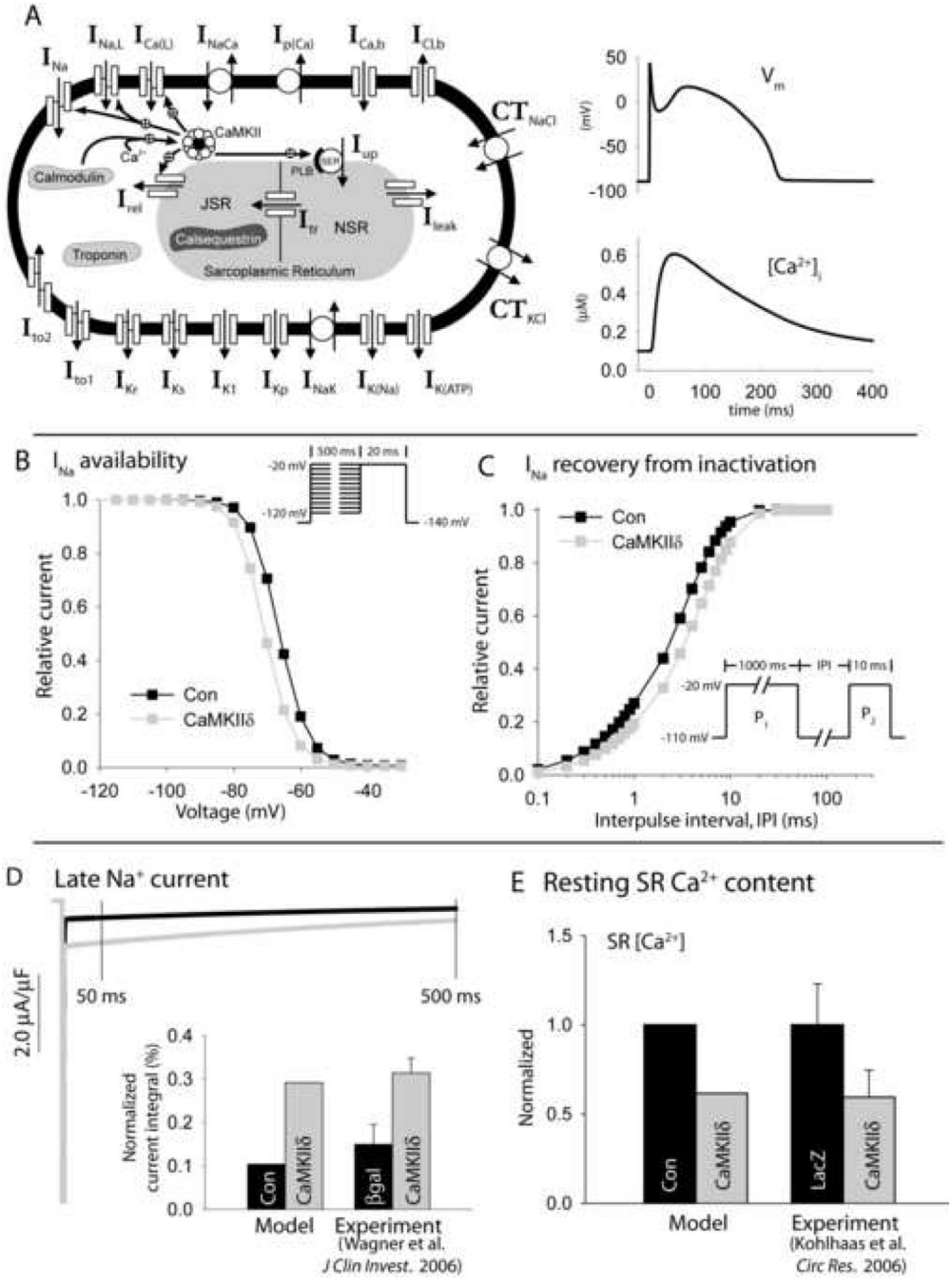

FIGURE 2. Mathematical model of cardiac action potential, calcium transient, and CaMKII regulatory pathway

(**A**) Updated Hund-Rudy dynamic (HRd) canine ventricular epicardial cell model (*left*). Symbols are defined in text and in Supplement Table S1. Simulated control (NZ) action potential and corresponding calcium transient for steady-state pacing at CL = 2,000 ms (*right*). (**B**) Simulated Na^+ channel availability (steady-state inactivation) in control model (Con, *black*) and in model with CaMKII hyperactivity (CaMKIIδ, *gray*). Pulse protocol shown in inset. (**C**) I_{Na} recovery from inactivation in control model (*black*) and with CaMKII hyperactivity (*gray*). Pulse protocol shown in inset. (**D**) Simulated late Na^+ current in control (*black*) and with CaMKII hyperactivity (*gray*) during a 500 ms voltage pulse to −20 mV from

a −140 mV holding potential. Simulated late Na^+ current integral (*inset*) is compared to experimental measurements [26] in rabbit ventricular myocytes overexpressing CaMKIIδ (*gray*) or β-galactosidase (βgal) as control (*black*). The late current is integrated from 50 to 500 ms and normalized to current integral in the absence of inactivation. (**E**) Simulated SR Ca^{2+} content in control model (*black*) and with CaMKII hyperactivity (*gray*) compared to experimental measurements [27] from rabbit myocytes overexpressing CaMKIIδ (*gray*) or LacZ as control (*black*).

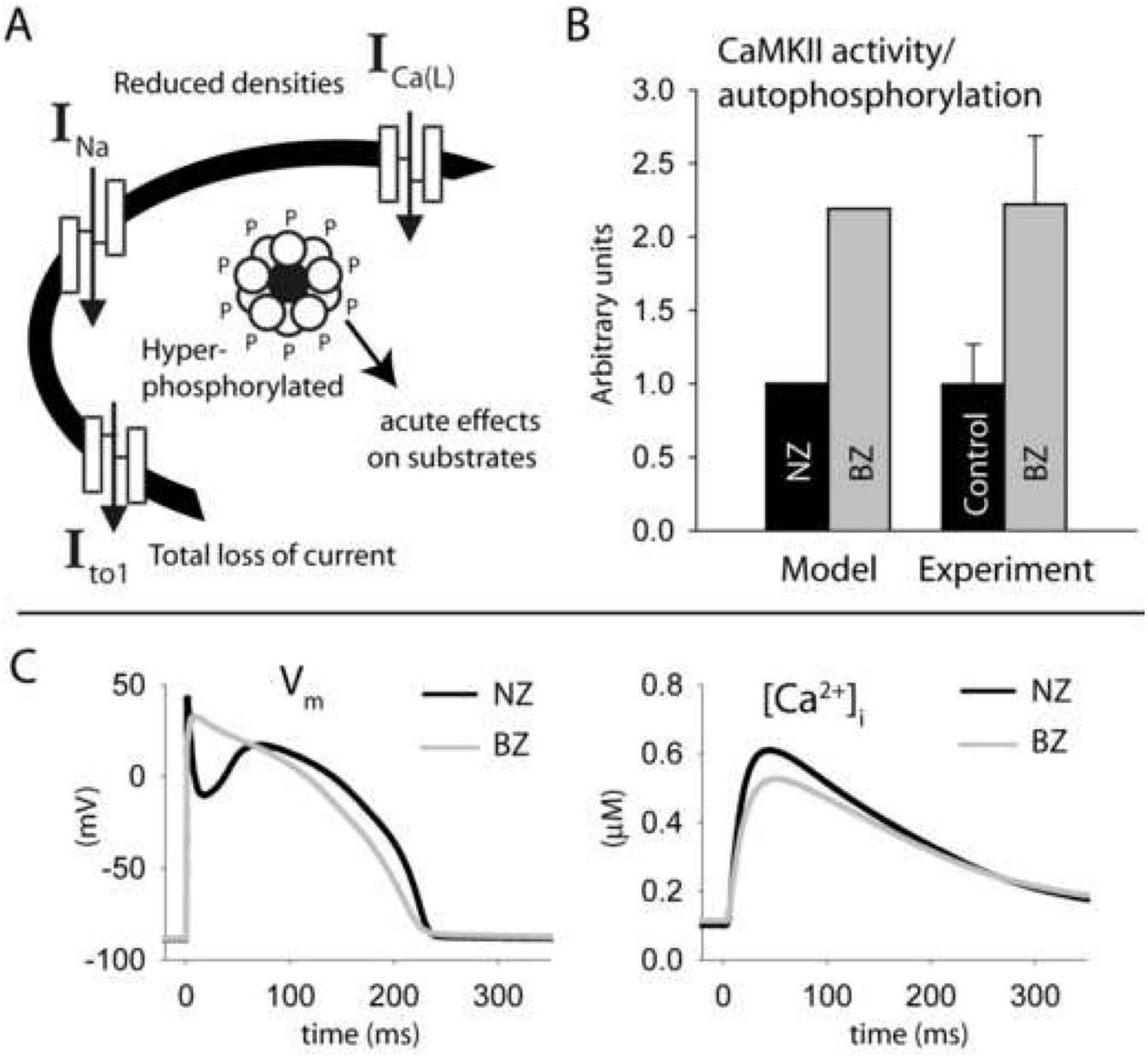

FIGURE 3. Mathematical model of infarct border zone myocyte

(**A**) Remodeling changes incorporated into the model include decreased $I_{Ca(L)}$, I_{Na}, and I_{to} densities and acute effects of CaMKII hyperactivity on downstream substrates. (**B**) Simulated basal CaMKII activity compared to experimentally measured autophosphorylation levels in NZ (*black bars*) and BZ (*gray bars*). Experimental data are from Figure 1B. (**C**) Simulated action potentials (*left panel*) and calcium transients (*right panel*) in NZ (control HRd model, *black line*) and BZ (*gray line*) models for steady-state pacing at CL = 2,000 ms.

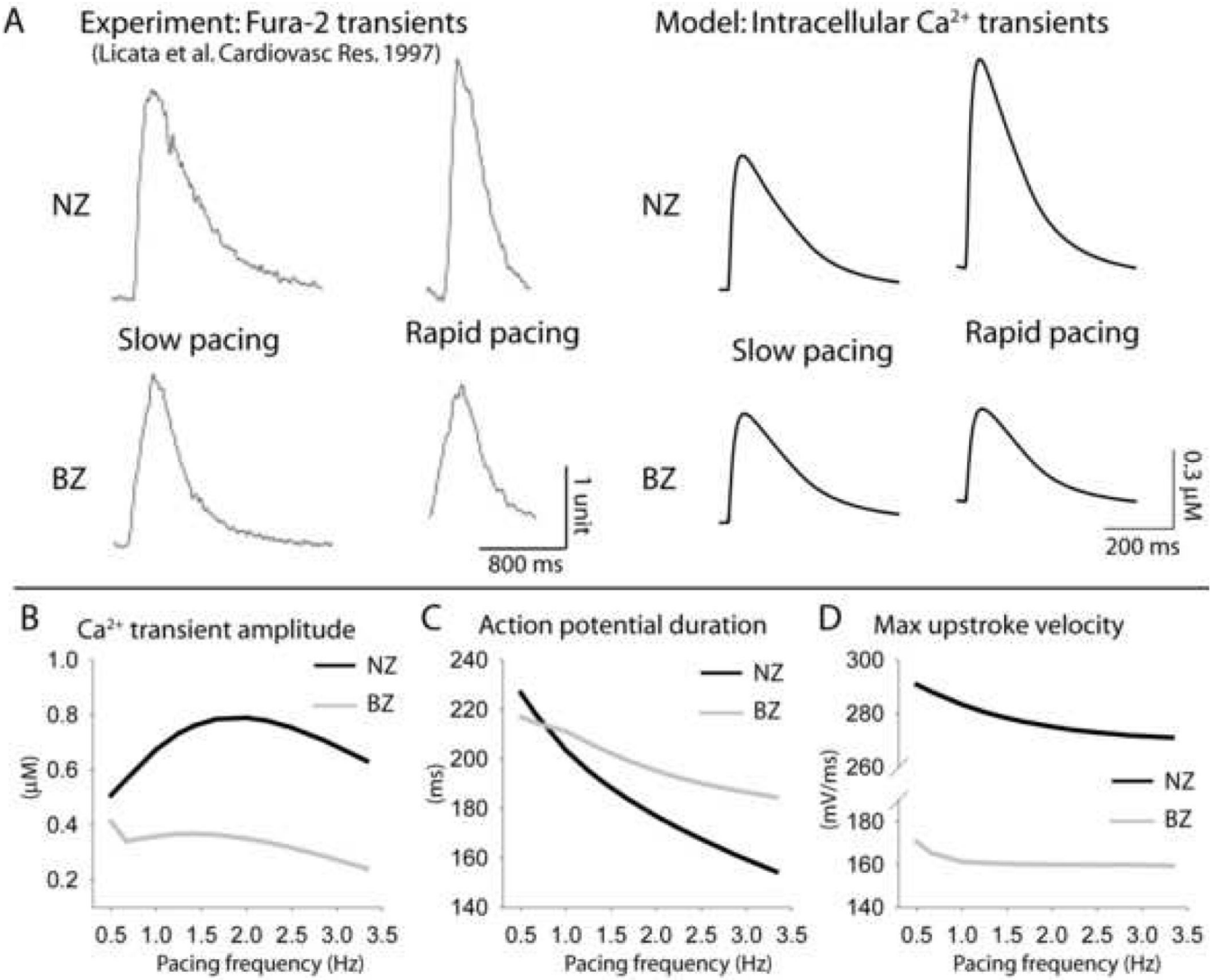

FIGURE 4. Altered action potential and calcium transient rate-dependent properties in border zone myocytes

(**A**) Normal zone (NZ) (*top*) and infarct border zone (BZ) (*bottom*) experimentally measured fura-2 transients (*left*) [38] and simulated Ca^{2+} transients (*right*) at slow and rapid pacing. Pacing CLs = 5,000 ms and 1,000 ms in experiments and 2,000 ms and 500 ms in simulations. Experiments were conducted at room temperature while model is based on data at 37°C. Simulated frequency dependence of (**B**) Ca^{2+} transient amplitude (CaT_{amp}), (**C**) action potential duration (APD), and (**D**) Maximal upstroke velocity in NZ (*black*) and BZ (*gray*) models.

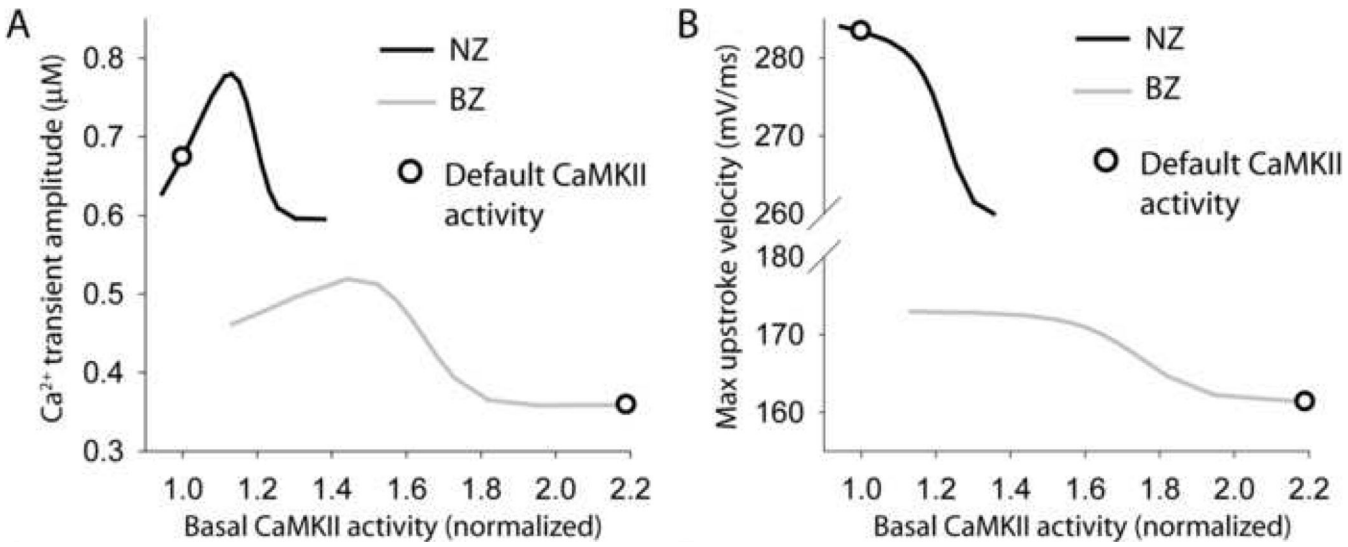

FIGURE 5. CaMKII-dependence of Ca^{2+} transient and action potential rate-dependent properties in normal and border zone myocytes

(**A**) Simulated steady-state (pacing frequency = 1 Hz) Ca^{2+} transient amplitude and (**B**) maximal upstroke velocity as a function of basal CaMKII activity in NZ (*black lines*) and BZ myocytes (*gray lines*). CaMKII autophosphorylation rate was altered to produce a range of basal CaMKII activities. Open circle on each curve indicates value corresponding to the default CaMKII activity.

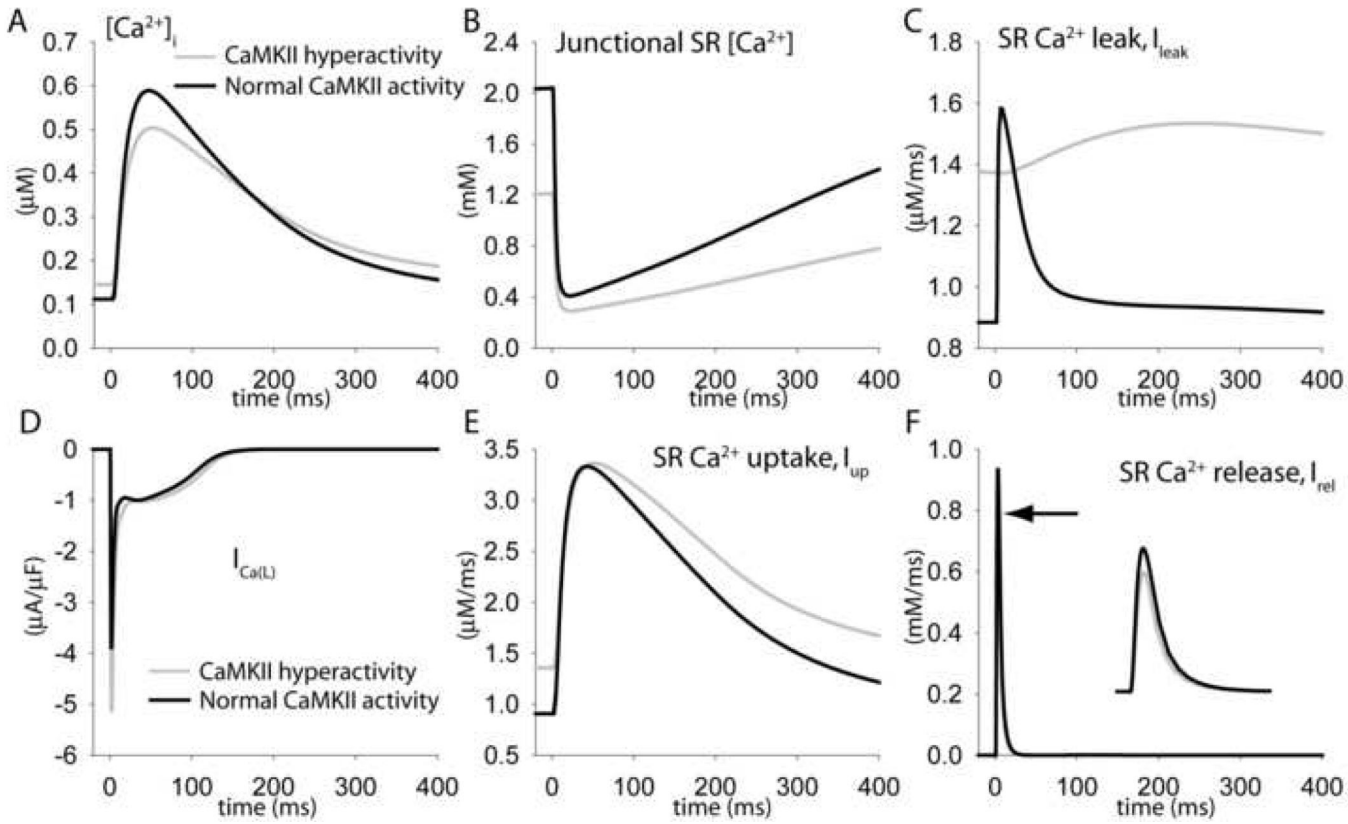

FIGURE 6. Increased SR Ca^{2+} leak due to CaMKII-hyperactivity decreases Ca^{2+} transient amplitude in BZ myocytes

Simulated steady-state (**A**) Ca^{2+} transients, (**B**) junctional SR [Ca^{2+}], (**C**) SR Ca^{2+} leak flux (I_{leak}), (**D**) L-type Ca^{2+} current, $I_{Ca(L)}$, (**E**) SR Ca^{2+} uptake flux (I_{up}), and (**F**) SR Ca^{2+} release flux (I_{rel}) in the default border zone model (including CaMKII hyperactivity, *gray lines*, *arrow* denotes peak) and in BZ model with basal CaMKII activity reduced to normal levels (*black lines*). Pacing frequency = 1 Hz.

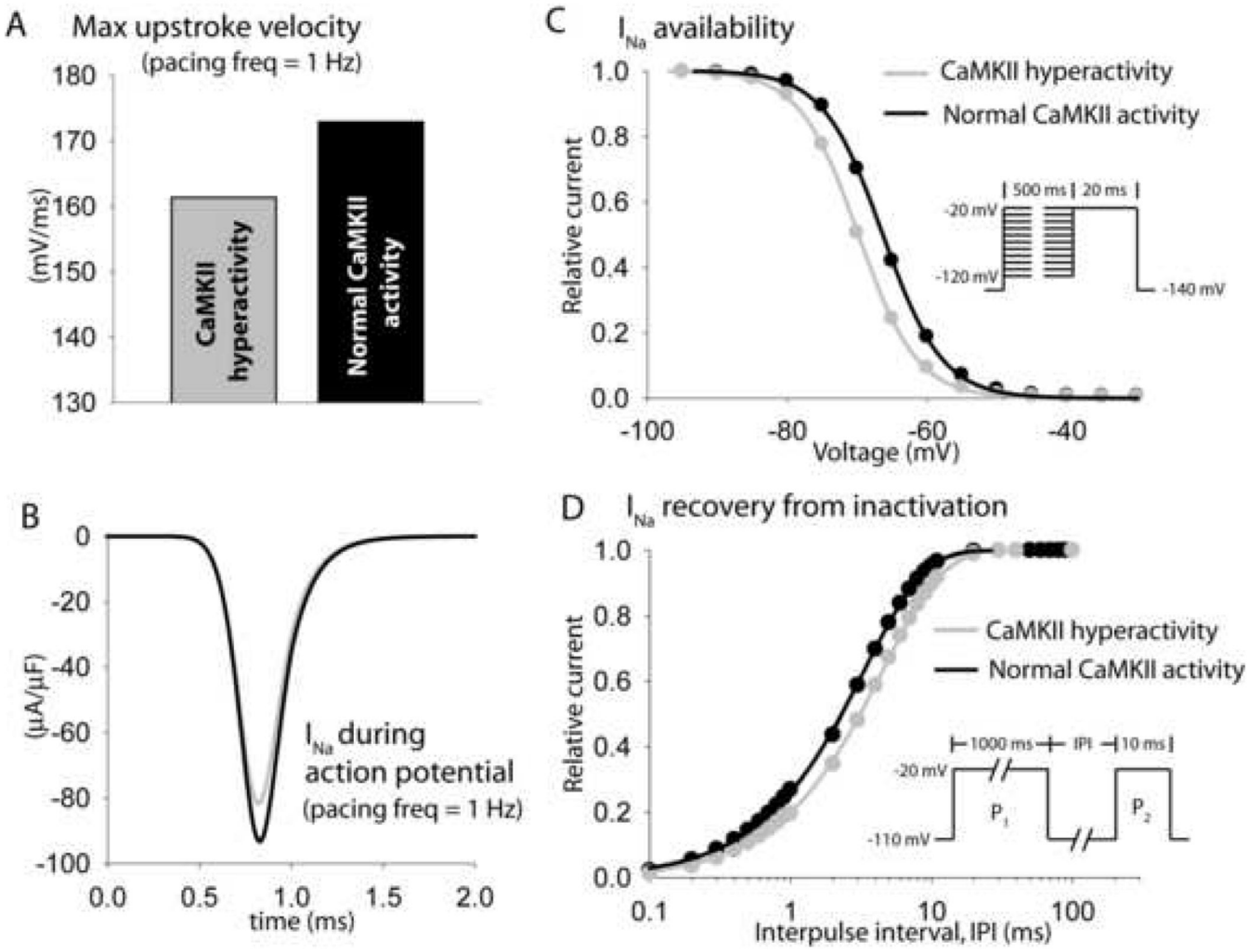

FIGURE 7. Altered Na^+ channel kinetics due to CaMKII-hyperactivity reduces upstroke velocity in BZ myocytes

Simulated steady-state maximal upstroke velocity and Na^+ current during the action potential in the default BZ model (including CaMKII hyperactivity, *gray lines*) and in BZ model with basal CaMKII activity reduced to normal levels (*black lines*). Pacing frequency = 1 Hz. (**C**) Simulated I_{Na} availability (steady-state inactivation) and (**D**) recovery from inactivation in the default border zone model (*gray lines*) and in BZ model with basal CaMKII activity reduced to normal levels (*black lines*). Pulse protocols are shown in inset.

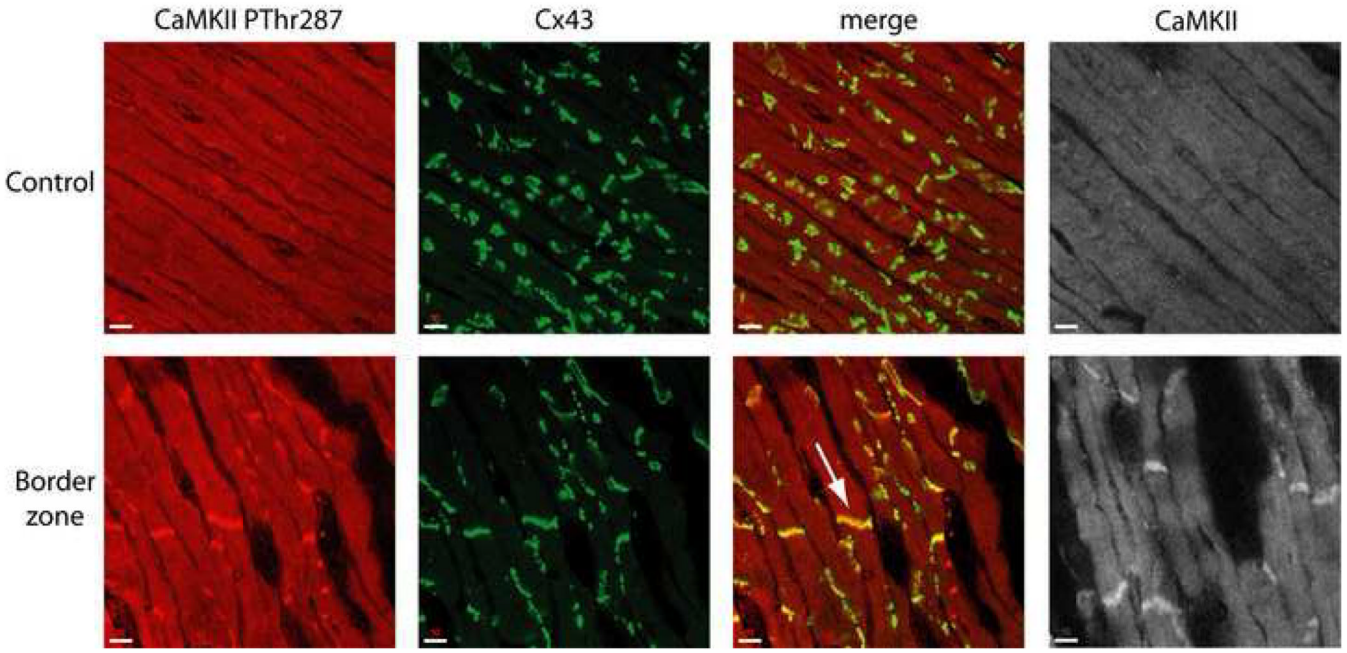

FIGURE 8. CaMKII localization increases at cell ends in the infarct border zone

Immunolocalization of CaMKII PThr287 (red, *far left*), connexin43 (Cx43) (green, *left of center*), and total CaMKII (gray, *far right*) in epicardial sections from control (*top*) and infarct border zone (BZ) (*bottom*) hearts. Merged images (*right of center*) are shown for CaMKII PThr287 and Cx43 double-labeling experiments indicating increased colocalization of CaMKII PThr287 and Cx43 at cell ends (*arrow*).